


# Microphase separation and thermo-mechanical properties of energetic poly(urethane–urea)

Jie Lv<sup>1</sup> · Jizhen Huo<sup>1</sup> · Ye Yang<sup>1</sup> · Yingfeng Yu<sup>1</sup>  · Guozhu Zhan<sup>2</sup> · Huikun Zhang<sup>2</sup>

Received: 4 May 2017 / Revised: 18 September 2017 / Accepted: 29 November 2017 /

Published online: 4 December 2017

© Springer-Verlag GmbH Germany, part of Springer Nature 2017

**Abstract** In this paper, the phase segregation and thermo-mechanical properties of energetic poly(urethane–urea) (EPUU) for propellant binder application are analyzed. Series of EPUUs are synthesized from copolymer of 3,3-bis-azido methyl oxetane and tetrahydrofuran, tolylene diisocyanate, and 3,3'-dichloro-4,4'-dianilino methane, with different hard segment contents ranging from 9.7 to 38%. With the enlargement of hard segment content from 9.7 to 28.9% (EPUU1–EPUU3), the percentage of ordered part via hydrogen-bonded C=O in urea increases as investigated by FTIR, further increase of hard segment content to 38% results in less hydrogen-bonded ordered part but more disordered part. The SAXS result also verifies the highest degree of phase segregation of EPUU3. The thermo-mechanical properties of energetic poly(urethane–urea) are related to the degree of microphase separation. With the increase of hard segment content, the tensile strength increases roughly, while the elongation at break drops from EPUU1 to EPUU4. EPUU3 exhibits the highest value of tensile strength and acceptable elongation at break.

**Keywords** Energetic · Poly(urethane–urea) · Microphase separation · Mechanical property

---

**Electronic supplementary material** The online version of this article (<https://doi.org/10.1007/s00289-017-2251-4>) contains supplementary material, which is available to authorized users.

---

✉ Yingfeng Yu  
yfyu@fudan.edu.cn

<sup>1</sup> State Key Laboratory of Molecular Engineering of Polymers, Collaborative Innovation Center of Polymers and Polymer Composite Materials, Department of Macromolecular Science, Fudan University, Shanghai 200433, China

<sup>2</sup> The 806th Institute of the Eighth Academy of CASC, Huzhou 313000, China

## Introduction

Modern solid propellants generally are composed of fuel particulate solid, oxidizers, explosives, plasticizer, and other auxiliaries. Fuel particulate solid, oxidizers, and explosives are as dispersed phase, and EPUUs obtained in our work are as continuous phase to bond them together firmly. Therefore, the mechanical properties of the propellant are appropriate to bear the load in storage, operation, ignition, and flight.

Energetic poly(urethane–urea) elastomers have already been used for solid propellant binder application for the last few decades. Among which, azide energetic binders show high potential because of its high amount of released heat, no oxygen consumption during decomposition, and decomposition products with low molecular weights [1]. Homopolymers and copolymers based on energetic  $-N_3$  group, represented by glycidyl azide polymer (GAP) [2], 3,3-bis-azido methyl oxetane (BAMO) [3, 4], and 3-azidomethyl-3-methyl oxetane (AMMO) [5] have been introduced into the elastomers. During decomposition and combustion, GAP binder produces relatively high concentrations of fuel fragments such as C(s),  $H_2$ , and CO because of low concentration of oxygen atoms within GAP binder. Combined with  $-N_3$  group, the addition of oxidizers within GAP binder increases the combustion potentials such as the specific impulse of rockets and the impetus of guns [6, 7].

GAP has a higher heat of formation; however, its mechanical properties are relatively poor with azido group. In Zhang et al.'s work, the highest tensile strength of GAP-based energetic thermoplastic elastomers did not reach 5 MPa and elongation was only 50% [2]. BAMO, with the presence of two symmetrical azido groups, cannot be used directly for binder application. One of the reasons is that large volume and strong polarity of side chain  $-CH_2N_3$  affect the flexibility of molecular chain and weaken two-stage cross-linking of the system, which leads to poor mechanical property [8, 9]. The other reason is that the melting temperature of BAMO is higher than curing temperature of poly(urethane–urea), and it is solid at room temperature [10, 11]. BAMO/AMMO copolymer binder has also been synthesized as double energetic binder, and different mechanical properties can be achieved by controlling polymer structures [5, 12]. However, the improvement in mechanical properties is limited and the cost is too high.

To solve the problems, copolymers composed of BAMO and tetrahydrofuran (THF) [13–15] with controlled molecular weight, low glass transition temperature and improved mechanical properties become excellent candidates for a binder system with high energy. At the present time, EPUU from BAMO/THF copolymer shows fine mechanical property at low temperature, however, still unsatisfactory at higher temperature.

Poly(urethane–urea), as well as energetic PUUs, consists of high glass temperature ( $T_g$ ) “hard” segment and low  $T_g$  “soft” segment. Since the former report of Cooper and Tobolsky [16], it is generally accepted that poly(urethane–urea) undergoes microphase separation due to incompatibility between the two segments. In the past years, many investigations have been applied to estimate the degree of separation, including spectroscopy [17, 18], SAXS [19–21], wide-angle

X-ray diffraction (WAXD) [22, 23], dynamic mechanical analysis (DMA) [24], and so on. To get quantitative results from differential scanning calorimeter (DSC), Camberlin et al. considered heat capacity change ( $\Delta C_p$ ) a parameter to estimate the degree of soft phase segregation, calculated by the ratio of  $\Delta C_p$  for the soft segment in PUUs and  $\Delta C_p$  for the pure soft segments at  $T_g$  [25]. Trovati et al. found that few crystallinity could be observed in the sample of soft PUUs, but the crystallinity increased from the soft, semi-rigid PUUs to rigid PUUs through WAXD [23]. Fourier transform infrared spectroscopy is very sensitive to hydrogen bonding, and a wide range of studies [26–29] agreed that the bands ranging from 3200 to 3400  $\text{cm}^{-1}$  corresponded to the bonded/free N–H region, 1690–1740  $\text{cm}^{-1}$  for C=O in urethane, while 1640–1690  $\text{cm}^{-1}$  for C=O in urea. Bonart et al. carried out detailed SAXS studies [30], which is known as a quantitative method applied to calculate the degree of microphase separation, domain purity, and boundary effect of PUUs.

Despite the numerous studies measuring microphase separation of PUUs, as far as we know, few of them applied the methodologies to the EPUUs analysis, even though microphase separation plays an important role in the mechanical properties of EPUUs [31–34]. The direct understanding of microphase separation in these energetic materials and its relationship with thermo-mechanical properties is the key to expand propellant binder application. In this paper, we employ the investigations combined of FTIR, SAXS, DMA, DSC, and tensile measurement for EPUUs, which synthesized from BAMO/THF, toluene diisocyanate (TDI), and 3,3'-dichloro-4,4'-diaminodiphenylmethane (MOCA), to obtain some insight of the microphase separation and thermo-mechanical properties of energetic poly(urethane–urea).

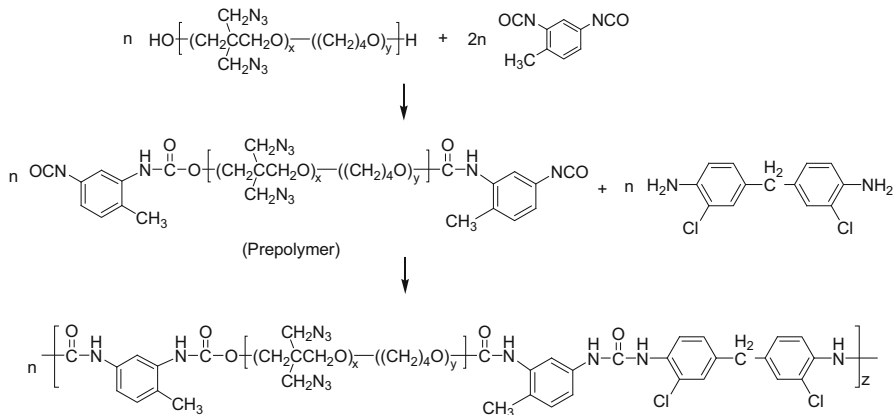
## Experimental

### Materials

A series of three-component poly(urethane–urea) EPUU comprising toluene diisocyanate (TDI 65/35, Bayer), BAMO/THF copolymer (the monomer ratio of BAMO to THF is 1:1, hydroxyl value 19.29 mg KOH  $\text{g}^{-1}$ ,  $M_n = 5143 \text{ g mol}^{-1}$ ,  $D = 2.80$ , Liming Research Institute of Chemical Industry, China) as soft segment, and 3,3'-dichloro-4,4'-diaminodiphenylmethane (MOCA, Aldrich) as chain extender were synthesized with different weight fractions of hard segment (MOCA and TDI). Dibutyltin dilaurate (DBTDL) was used as a catalyst. BAMO/THF copolymer was dehydrated in vacuum before use. The chemical structure of EPUU from BAMO/THF–TDI–MOCA is given in Scheme 1.

### Sample preparation

A two-step reaction was used in our experiment. The first step was to obtain the pre-polymer by BAMO/THF and TDI. The reaction was conducted under nitrogen in a three-necked flask. Upon BAMO/THF stirring at 60 °C, TDI was added. After 4 h reaction period, pre-polymer was obtained and further stored in refrigerator. The



**Scheme 1** Scheme of the reaction and chemical structure of EPUU1 by the two-step “pre-polymer” method

second step was the reaction of pre-polymer and chain extender. MOCA was dissolved in toluene and mixed with pre-polymer with the amount by designed hard segment weight fraction, which was calculated by the percentage of all TDI and MOCA units in gross weight, as shown in Table 1. The polymeric solutions were poured into tetrafluoroethylene mold and cured at 100 °C for 12 h and at room temperature for 7 days. Then, films of EPUUs were obtained with the thickness of about 0.5 mm and were cut into different standard sizes for further tests.

## Experimental methods

### FTIR

Fourier transform infrared spectrometer was used to track reaction process upon mixing of pre-polymer and MOCA. The mixture was cast onto potassium bromide

**Table 1** Composition and glass temperature of EPUUs

Name	Ratio <sup>a</sup>	hard segment wt% <sup>b</sup>	$T_g$ by DSC (°C) <sup>c</sup>	$T_g$ by DMA (°C) <sup>c</sup>	$T_g$ by DMA (°C) <sup>d</sup>
BAMO/THF			– 54		
EPUU1	1:2:1	9.7	– 39	– 36	–
EPUU2	1:4:3	20.4	– 44	– 38	–
EPUU3	1:6:5	28.9	– 46	– 40	165
EPUU4	1:8:7	38	– 48	– 44	177
TDI + MOCA			<sup>d</sup> 198		

<sup>a</sup> –OH/NCO/NH<sub>2</sub> molar ratio

<sup>b</sup> Hard segment content

<sup>c</sup>  $T_g$  of the soft segment

<sup>d</sup>  $T_g$  of the hard segment

pellet. Thermo Nicolet 6700 Spectrometer (ThermoFisher, America) with  $4\text{ cm}^{-1}$  resolution and 128 scans was chosen in our experiment.

### *DSC*

Differential scanning calorimeter experiments were carried out using instruments Q2000 (TA, America). The scanning range was from  $-80$  to  $220\text{ }^{\circ}\text{C}$  under nitrogen atmosphere. The heating and cooling rate was  $10\text{ }^{\circ}\text{C min}^{-1}$  and was realized by mechanical refrigeration. The sample weight was about 5–8 mg.  $T_g$  reported was taken from the second heating process.

### *DMA*

Data of dynamic mechanical analysis were obtained using DMA SDTA861e (Mettler Toledo, Switzerland). The scanning range was from  $-80$  to  $200\text{ }^{\circ}\text{C}$  under air atmosphere, with a heating rate of  $5\text{ }^{\circ}\text{C min}^{-1}$ . Samples with dimension of  $10\text{ mm} \times 4\text{ mm} \times 0.2\text{ mm}$  were measured in tensile mode at an oscillation frequency of 1 Hz. Storage modulus ( $E'$ ) and loss factor ( $\tan\delta$ ) were measured, and  $T_g$  was defined as the temperature corresponding to the maximum value of the  $\tan\delta$ .

### *SAXS*

Small angle X-ray scattering experiments were performed at the NanoStar U SAXS System (Bruker, Germany) using  $\text{Cu}_{K\alpha}$  radiation (40 kV, 35 mA, wave length  $\lambda = 1.5418\text{ \AA}$ ). The data window was from  $0.2^{\circ}$  to  $2.8^{\circ}$ .

### *Mechanical test*

The stress–strain measurements were performed using CMT4104 testing machine (China). After remaining at  $25\text{ }^{\circ}\text{C}$  for 24 h, the dumbbell specimens ( $L_0$  with 15 mm) were then stretched using extension rate  $50\text{ mm min}^{-1}$  and force 50 N, respectively. Typically, the data reported from the test were the mean value of five specimens.

## **Results and discussion**

### **FTIR in situ monitoring microphase separation**

#### *Curing process*

The change of functional groups of EPUU1 during curing was monitored in situ by time-dependent FTIR investigation lasting for 0.5 h, as presented in Fig. 1. The change in the C = O region of this series of EPUUs reflecting the extent of microphase separation was provided in supplementary information Fig. S1.

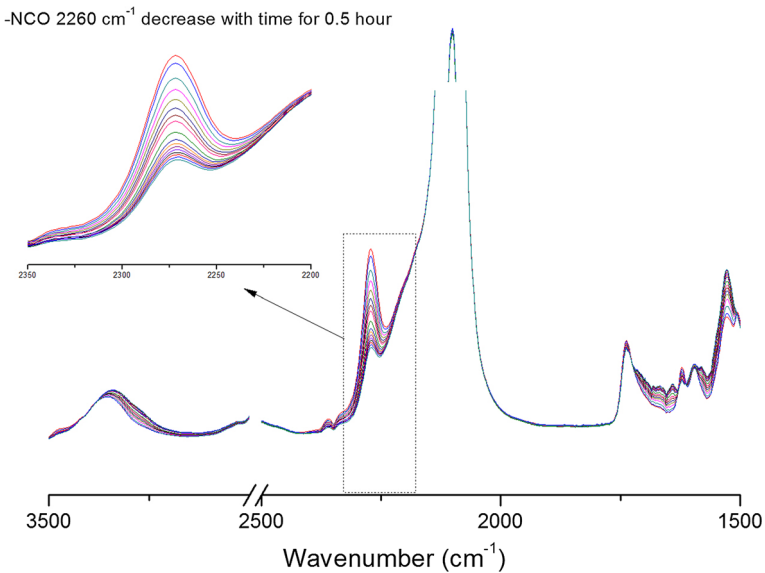


**Fig. 1** Time-dependent change of the FTIR spectra for EPUU1 in 0.5 h

With the reaction of  $\text{-NCO}$  and  $\text{-NH}_2$ , there were obvious increases in the peak intensity from  $1640$  to  $1690\text{ cm}^{-1}$  in urea. Not only grew the peak intensity in urea groups, but also the percentage of urea area increased from EPUU1 to EPUU4. However, the absorption peak at  $1740\text{ cm}^{-1}$  of free  $\text{C=O}$  group in urethane decreased with the curing because of H bonding. Interestingly, the peak at  $1715\text{ cm}^{-1}$ , hydrogen-bonded disordered  $\text{C=O}$  in urethane, first ascended and then descended in 0.5 h. The phenomenon met agreement with the Yilgor's study [27], in which time-dependent FTIR spectra between  $1675$  and  $1750\text{ cm}^{-1}$  were analyzed by deconvolution of the  $\text{C=O}$  peaks using the Peakfit Version 4.12 software, to determine the peak area of specific  $\text{C=O}$  compared with the total peak area as percent amount. In their analysis,  $1733$ ,  $1708$ , and  $1696\text{ cm}^{-1}$  were assigned as free, hydrogen-bonded disordered and ordered, while their percentage separately decreased, first ascended and then descended, increased through the curing. At the end of the curing process, the peak intensity at  $1696\text{ cm}^{-1}$  was also defined as the well-separated hard segments and peak at  $1733\text{ cm}^{-1}$  was defined as the mixed part with soft matrix in the study. In our work, peak fitting by Matlab was also used (Fig. 2), combined with the following equation, to obtain the percentages of free, hydrogen-bonded disordered and ordered  $\text{C=O}$  groups in urethane and urea:

$$\begin{aligned}
 C &= O(1640)\% \\
 &= A(1640)/A(1640) + A(1660) + A(1680) + A(1695) + A(1713) + A(1740) \cdot
 \end{aligned}
 \tag{1}$$

The peak integration results for the FTIR spectrum (Fig. 3) are provided in Table 2. After the reaction of 7 days and 12 h, actual relative percentage of entire urea area

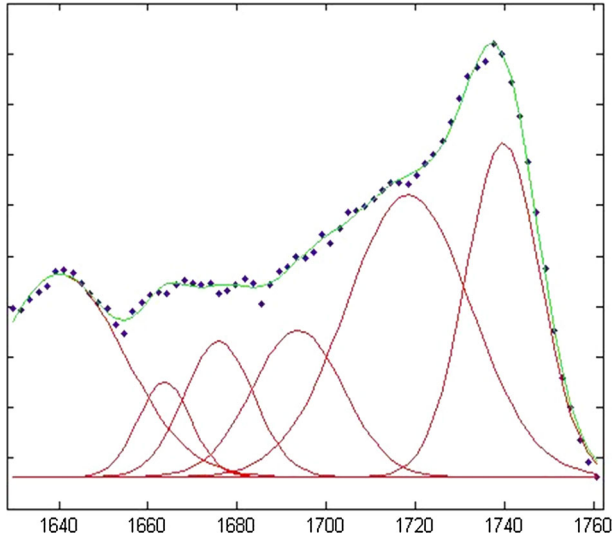


**Fig. 2** Peak fitting by Matlab in C=O region of the FTIR spectra

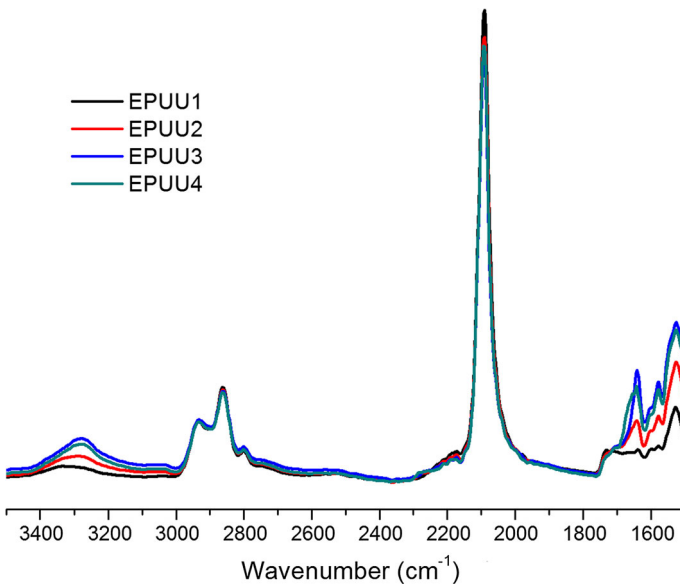


**Fig. 3** FTIR spectra for EPUUs after curing

(1640, 1662, and 1680  $\text{cm}^{-1}$ ) increased from EPUU1 to EPUU4, but maintained almost the same between EPUU3 and EPUU4, even though the hard segment mixture ratio was different upon mixing. More precisely in the hydrogen-bonded ordered band 1640  $\text{cm}^{-1}$  in urea region, the relative area was 19% for EPUU1, 30% for EPUU2, 48% for EPUU3, but 35% for EPUU4, in which intensity concentrated

**Table 2** Quantitative analysis in the C = O region of the FTIR spectra

Series	Relative absorbance of C=O groups in urea			Relative absorbance of C=O groups in urethane		
	1640 cm <sup>-1</sup> (%)	1662 cm <sup>-1</sup> (%)	1680 cm <sup>-1</sup> (%)	1695 cm <sup>-1</sup> (%)	1715 cm <sup>-1</sup> (%)	1740 cm <sup>-1</sup> (%)
EPUU1	19	4	8	13	33	23
EPUU2	30	11	15	20	15	9
EPUU3	48	4.5	9.5	18	15	5
EPUU4	35	22	7.7	8.2	20	7.1

on hydrogen-bonded order 35% and hydrogen-bonded disorder 22%. The previous studies of Yilgor [27], Tereshatov and co-workers [35–38] treated the relative intensity of hydrogen-bonded ordered band as the indicator of microphase-separated hard segments. In our research, we temporarily followed the criterion regarding EPUU3 as the poly(urethane–urea) with maximum percentage of microphase separation, and verified with more measurement and theory.

### Band assignment

The band assignment discussed above was based on the previous studies and our actual work. According to former studies [27, 28, 39], bands ranging from 1690 to 1740 cm<sup>-1</sup> correspond to the hydrogen-bonded/free C=O in urethane while 1640–1690 cm<sup>-1</sup> for C=O in urea. Ishihara et al. [40], Park Sung et al. [41], and Ning et al. [42] utilized FTIR measurement to investigate the absorption bands of poly(urethane–urea). For the urethane groups, 1729–1739 cm<sup>-1</sup> was assigned to the free C=O and 1706–1713 cm<sup>-1</sup> for hydrogen-bonded C=O, while bands at 1691 and 1666 cm<sup>-1</sup> were related to free and hydrogen-bonded disordered C=O and 1643–1628 cm<sup>-1</sup> for hydrogen-bonded ordered C=O in urea groups, separately. On the bases of that, Tereshatov and co-workers conducted a series of studies focusing on poly(urethane–urea), including copolymer based on TDI, MOCA, and oligotetramethylene oxide diol (PTMO) [35–38]. Compared with study of Ning et al., the conclusion was similar, but further refined band at 1692–1693 cm<sup>-1</sup> to both hydrogen-bonded, ordered C=O of urethane and free C=O of urea groups in their study. In our work, the corresponding peak position was defined, as shown in Table 2 and supplementary information Fig. S2.

### SAXS Analysis of microphase separation

Information about the relative percent of intermixing effect, boundary effect, and degree of microphase separation of EPUUs was provided by SAXS measurement, as presented in Fig. 4. The ideal two-phase separation was considered with sharp boundaries, the blue domain represents the hard segment, and the white part



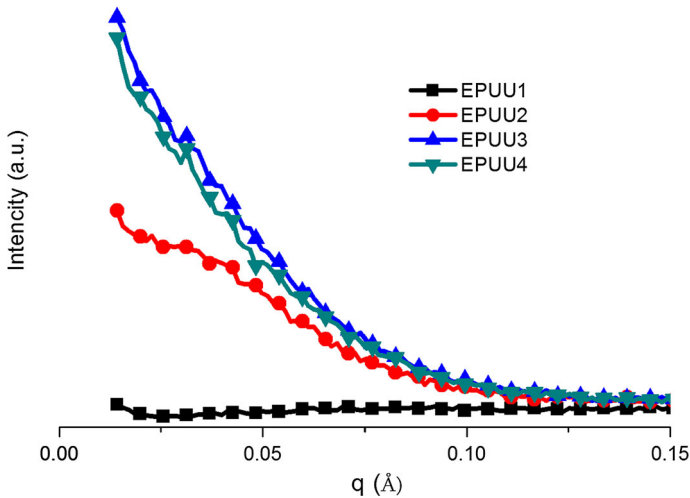


**Fig. 4** Scattered intensity  $I(q)$  versus  $q$  for EPUUs

represents soft segment, as shown in Fig. 5c. In addition, the theoretical electron density  $\Delta\eta_0^2$  is calculated by the following:

$$\Delta\eta_0^2 = \emptyset_{hs}(1 - \emptyset_{hs})(\eta_{hs} - \eta_{ss})^2, \tag{2}$$

where  $\emptyset$  represents volume fraction and  $\eta$  means theoretical electron density of the hard or soft segment, respectively.

In our study, all TDI and MOCA were counted as the hard segment, according to Bonart and Muller’ theory [30]. In addition, the electron density  $\eta$  was calculated with the guide of group contribution approach [43]. The electron density of pure hard segment TDI–MOCA was calculated to be 1.760 g/cm<sup>3</sup> and soft segment to be 1.364 g/cm<sup>3</sup> in our study. In the previous work, the density of 4,4’-methylene di(p-phenyl isocyanate) (MDI)-based hard segment system has once been calculated, such as MDI–butanediol (BDO) hard segment with 1.354 g/cm<sup>3</sup> in Leung’ work [20], MDI–ED hard segment with 1.424 g/cm<sup>3</sup> [21]. However, as far as we know, there is no similar report once reported comparable result with our research.

In a real EPUU system, the boundaries between two phases are indistinct, as presented in Fig. 5a, which contain diffuse phase boundaries and mixing domain. In this case, the actual electron densities decreased compared to the ideal system. There, background can be first corrected, corresponding to the model shown in Fig. 5a, calculated by the SAXS data using the following formula:

$$\Delta\eta^2 = c \int_0^\infty [I(q) - I_b(q)]q^2 dq, \tag{3}$$

where

$$c = 1/2\pi^2 i_e N_A^2 = 1.76 \times 10^{-24} \text{ mol}^2/\text{cm}^2.$$

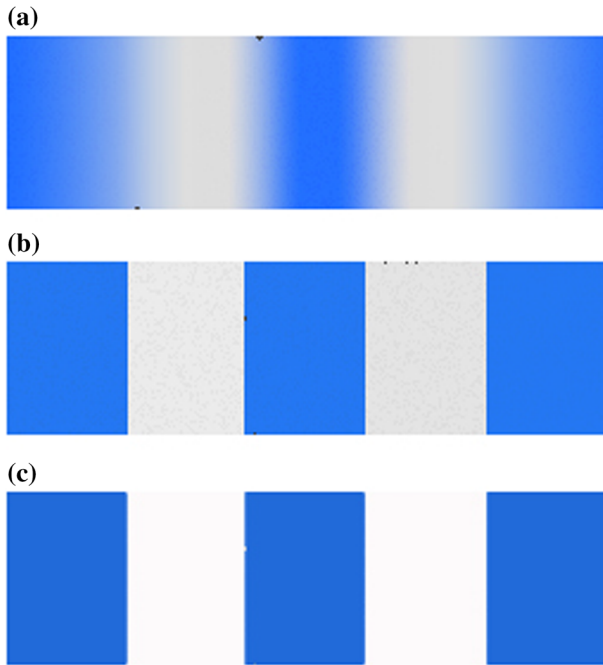


**Fig. 5** Characteristic electron density differences. Hard segments are blue, and soft segments are white. **a** Real system including contributions from diffuse boundaries and mixing domains; **b** system with domain mixing but no diffuse boundary; **c** ideal electron density difference

The effects of diffuse phase boundaries can be further corrected as well, supported by Koberstein et al.'s work [44], and leaves only gray regions representing phase mixing, as shown in Fig. 5b:

$$\Delta\eta^{2''} = c \int_0^\infty [I(q) - I_b(q)]q^2/H^2(q)dq, \quad (4)$$

where

$$H^2(q) = \exp[-1.36(\sigma q)^{1.81}], \quad (5)$$

and  $-\sigma^2$  is determined from the slope of a  $\ln[(I(q) - I_b(q))q^4]$  versus  $q^2$  plot.

The ratio of the background corrected experimental variance to the theoretical electron density of ideal phase separation  $\Delta\eta^{2'}/\Delta\eta_0^2$  is defined as the degree of overall microphase separation. The parameter  $(\Delta\eta_0^2/\Delta\eta^{2''}) - 1$  is used to calculate effect of domain mixing. Finally,  $(\Delta\eta^{2''}/\Delta\eta^{2'}) - 1$  gives information about the boundary diffuseness. As we do not focus on the boundary thickness in this paper, values to estimate degree of overall microphase separation are presented in Table 3, showing 3% for EPUU1, 15% for EPUU2, 21% for EPUU3, and 17% for EPUU4. Actually, the separation is not that complete compared to our common sense that EPUUs are well phase-separated materials. Koberstein et al. once investigated the

**Table 3** Electron density variance ratios for EPUUs

Series	Hard segment (%)	$\Delta\eta_0^2$ (mol e <sup>-</sup> /cm <sup>3</sup> ) <sup>2</sup>	$\Delta\eta^{2'}$ (mol e <sup>-</sup> /cm <sup>3</sup> ) <sup>2</sup>	$\Delta\eta^{2'}/\Delta\eta_0^2$ Phase separation
EPUU1	9.7	$2.385 \times 10^{-3}$	$7.145 \times 10^{-5}$	0.03
EPUU2	20.4	$4.421 \times 10^{-3}$	$6.841 \times 10^{-4}$	0.15
EPUU3	28.9	$5.594 \times 10^{-3}$	$1.155 \times 10^{-3}$	0.21
EPUU4	38	$6.414 \times 10^{-3}$	$1.100 \times 10^{-3}$	0.17

microphase separation of two PUUs with hard segment content of 22% [44]. One is composed of 50/50 mixture of polypropylene ether diol (MW = 8300) and polypropylene ether triol (MW = 7475) as soft segment and TDI-ED as hard segment; the other consists of polypropylene ether triol (MW = 10,000) as soft segment and MDI-BDO as hard segment. The SAXS measurement revealed that degree of microphase separation of TDI-ED system was about 30%, while the MDI-BDO was 40%, due to the better symmetry of MDI. In our study, the overall degree of separation is lower than that of TDI-ED system in Koberstein et al.'s work, which may be caused by the poorer symmetry of TDI/MOCA. Notably, the general trend observed by SAXS corresponded to that by FTIR: EPUU3 gained the highest degree of microphase separation and may achieve optimal mechanical properties with lower phase mixing influence and boundary diffuseness.

## Thermal–mechanical properties

### DSC test

The thermal–mechanical properties represented by  $T_g$ , storage modulus, elasticity, and tensile strength of EPUUs were investigated by the combination of DSC, DMA, and tensile test. DSC first put insight into glass temperature of the system, as exhibited in Fig. 6.  $T_g$  of soft segment in EPUUs is summarized in Table 1.  $T_g$  of pure soft segment (BAMO/THF) was approximately at  $-54$  °C, which promises the application of EPUUs at low temperature. The relationship between  $T_g$  of soft segment and microphase separation was once discussed in Camberlin's work [25].  $T_g$  shift was considered a qualitative parameter to determine the degree of soft phase segregation, as the closer between  $T_g$  of EPUUs and pure soft segment, the fewer soft segment mixed in hard segment or at interphase. Heat capacity change at  $T_g$  was also reported in their work as a quantitative method. In our study,  $T_g$  was  $-39$ ,  $-44$ ,  $-46$ , and  $-48$  °C with the increase of hard segment content, indicating that soft segment intended to self-associate to form soft domain instead of mixing in the hard segment, which contributed to the increased percent segregation and closer  $T_g$  of soft phase.  $T_g$  of pure hard segment (TDI + MOCA) was located at  $198$  °C, which was similar to  $T_g$  of TDI and ethylenediamine (ED); Paik Sung et al. once investigated in their study of  $203$  °C [45]. From the DSC scans, information about  $T_g$  of hard segment in EPUUs material was unavailable. Because the change in heat

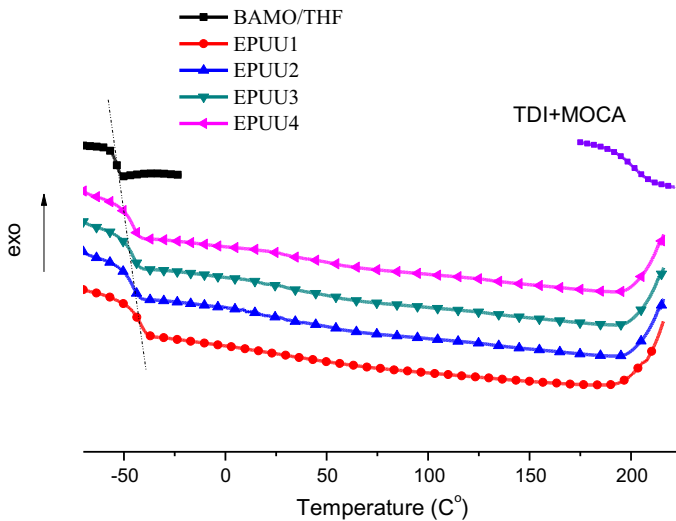


**Fig. 6** DSC scans of EPUUs, pure soft segment and hard segment

capacity of hard segments in EPUU is often small to detect [25, 46] and  $T_g$  was very closed to decomposition temperature according to our investigation.

#### DMA test

$T_g$  and storage modulus were further measured by DMA, as illustrated in Fig. 7 and summarized in Table 1. These curves are similar to the work by Stanford et al. [47], in which phase separation of co-polyurethanes was studied. In our work, two major transitions indicating the soft and hard segment glass transitions were observed of EPUU3 and EPUU4, at temperatures around  $-40$  and  $160$  °C. However,  $T_g$  of hard segment was unavailable of EPUU1 and EPUU2, as it was very close to the decomposition temperature according to the DMA curve.

The  $T_g$  values of soft segment were  $-36$ ,  $-38$ ,  $-40$ , and  $-44$  °C from EPUU1 to EPUU4, with a very small deviation in numerical value from that in the DSC test, which is caused by the different principles both methods based on. However, the trend that  $T_g$  getting closer with the pure soft segment with the increasing hard segment verified the DSC analysis. In storage modulus curve, the plateau after  $T_g$  indicated the intensity of physical crosslinks in EPUUs, and the modulus after  $T_g$  increased from EPUU1 to EPUU4 as observed. With the increase of hard segment content, interconnectivity of hard segment domains became stronger, which developed a continuous hard microdomain structure (hydrogen-bonded ordered part and hydrogen-bonded disordered part) to provide a significant structural reinforcement. For EPUUs, modulus enhanced with hard segment increasing, proving by the  $T_g$  shift and the crosslink intensity. However, the gap between EPUU3 and EPUU4 has diminished. The  $T_g$  values of hard segment were  $165$  and  $177$  °C of EPUU3–EPUU4 separately, but no visible signal was seen in the

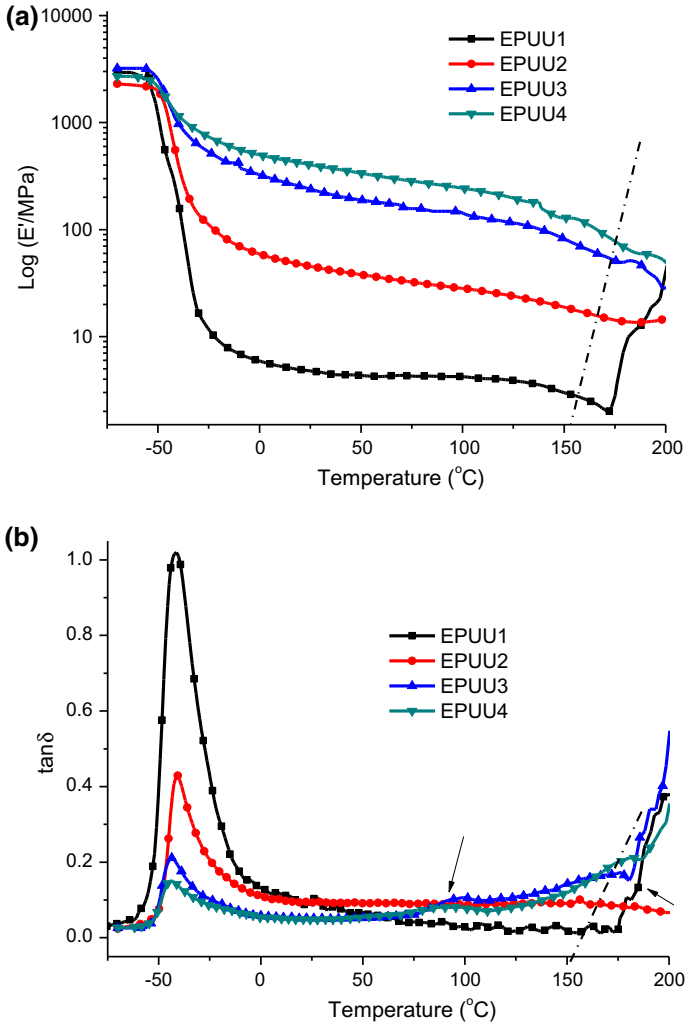


**Fig. 7** DMA test for a series of EPUUs **a** storage modulus; **b**  $\tan\delta$

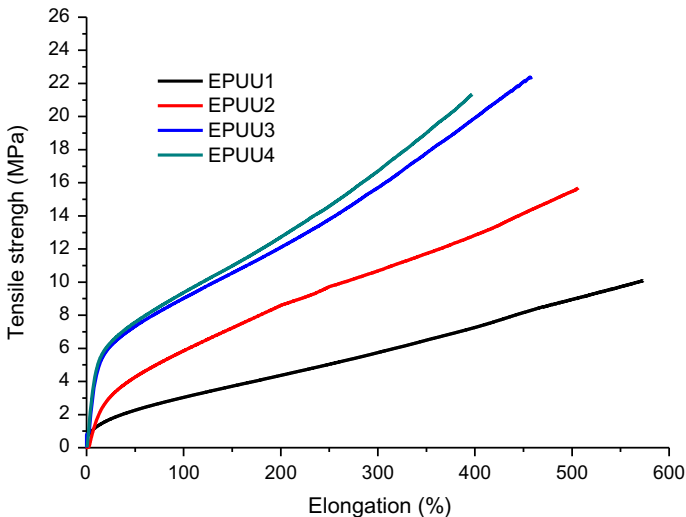
EPUU1 and EPUU2 curve. The purity of hard domain seemed to increase with the increase of hard segment percentage, as evidenced by more closely and obvious  $T_g$  of EPUU4 to pure hard segment, resulting by more thorough separation of hard domain.

*Tensile test*

The mechanical performance of EPUUs as an average result of five specimens investigated by tensile test is presented in Table 4, examples of the tensile curves in Fig. 8. On one hand, the elongation at break dropped from EPUU1 to EPUU4 with the soft segment decrease, which provided the elasticity. On the other hand, the

**Table 4** Mechanical properties of EPUUs

	EPUU1	EPUU2	EPUU3	EPUU4
Elongation at break (%)	587 ± 58 <sup>a</sup>	469 ± 60	437 ± 29	374 ± 65
Tensile strength (MPa)	10 ± 3	15 ± 3	22 ± 2	21 ± 2

<sup>a</sup>Standard deviation**Fig. 8** Examples of the tensile curves

tensile strength increased due to the increasing amount of urea groups from EPUU1 to EPUU3, and remained equal level with EPUU4. The phenomenon can be explained that with the increase of urea, more intermolecular interactions, and hydrogen bonding formed, which was considered as physical cross-linking. However, tensile strength and hard segment strength did not increase with the same frequency, and a slight drop can be observed in EPUU4. In this case, the optimal choice is EPUU3, which exhibited higher values of tensile strength but only a slight decrease in elongation at break.

The influence of several factors on tensile properties of various PUUs has been investigated by Yilgor, Wilkes, and co-workers, as comprehensively summarized by Wilkes et al. [34]. In Wilkes et al.'s study, poly(propylene oxide)glycol (PPG) (Mn of 11,800 g/mol) was used as soft segment, bis(4-isocyanatocyclohexyl)methane (HMDI), and 2-methyl-1,5-diaminopentane diamine (DY) as the chain extender. A series of poly(urethane–urea)s with hard segment contents of 12–30 wt% were synthesized, and the tensile strength increased from 4.6 to 20.9 MPa, and the elongation decreased from 1470 to 990% [48]. Wilkes et al. also measured the thermal properties of linear PUUs containing 28 wt% hard segment content synthesized by HMDI, DY, and poly(propylene oxide) (PPO) with different (Mn)

values of 2030, 4040, 8000, and 11,800 g/mol [49]. The tensile strength and elongation of copolymers utilized in this study ranged from 10 to 22 MPa and from 1200 to 1000%, respectively. Compared with the results in our study, the tensile strength from 10 to 22 MPa was similar to the results of Wikes et al., while the elongation from 587 to 374% was lower than that of Wikes et al. As it is known, the thermal and mechanical properties of PUUs are influenced by many factors, including soft segment type, molecular weight, hard segment type, and content; EPUUs in our study exhibited relatively high values of tensile strength and acceptable elongation at break based on its own specific structure.

For EPUUs in our work, the soft segment BAMO/THF provided elasticity mainly, while hard segment of TDI/MOCA units acted as physical cross-linking and gained stiffness of the material. For EPUU1 and EPUU2, no clear transition of hard segment was observed by DMA. This phenomenon could be due to higher phase mixing. Thus, similar elongation at break and tensile strength was observed of EPUU1 and EPUU2, resulting by few hard segments separated and formed continuous domain. As shown by DMA curve for EPUU3 and EPUU4, significant phase separation was existed, which was conformed by the detection of  $T_g$  of hard segment. It was coincident with the SAXS result and FTIR analysis that degree of phase separation was increase with the increased hard segment content. The tensile strength of EPUU3 and EPUU4 was highly improved compared to EPUU2, confirming that hard domain formed and acted as physical cross-linking. Although the elongation at break drops from EPUU1 to EPUU4, EPUU3 exhibited the highest value of tensile strength and acceptable elongation at break.

## Conclusions

Series of energetic poly (urethane urea) copolymers with different hard segment contents were synthesized, and their microphase separation was investigated by the combination of FTIR, SAXS, DSC, DMA, and tensile test.

With the increase of hard segment, the percentage of urea group increased, which consists of hydrogen-bonded ordered part and hydrogen bonding disordered part. Hydrogen-bonded ordered part of EPUU3 was 48% as investigated by FTIR, higher than EPUU1 and EPUU2 with less urea group, also higher than EPUU4, which has 35% hydrogen-bonded ordered part only but more disordered part. The result in SAXS, which accorded with the above, showed that the degree of microphase separation of EPUU3 was higher than EPUU4. The hydrogen-bonded ordered part may contribute to the phase separation.

With the increase of hard segment content, the tensile strength increases roughly, while the elongation at break drops from EPUU1 to EPUU4, and EPUU3 exhibited the highest value of tensile strength and acceptable elongation at break. Thermal–mechanical properties of EPUUs were related to the content of hydrogen-bonded ordered part, but not the content of hard segment.

**Acknowledgements** This research work was supported by the SAST Foundation No. 2015101.

## References

1. Pisharath S, Ang HG (2007) Synthesis and thermal decomposition of GAP-Poly(BAMO) copolymer. *Polym Degrad Stabil* 92(7):1365–1377. <https://doi.org/10.1016/j.polymdegradstab.2007.03.016>
2. Zhang ZJ, Wang G, Wang Z, Zhang YL, Ge Z, Luo YJ (2015) Synthesis and characterization of novel energetic thermoplastic elastomers based on glycidyl azide polymer (GAP) with bonding functions. *Polym Bull* 72(8):1835–1847. <https://doi.org/10.1007/s00289-015-1375-7>
3. Badgujar DM, Talawar MB, Asthana SN, Mahulikar PP (2008) Advances in science and technology of modern energetic materials: an overview. *J Hazard Mater* 151(2–3):289–305. <https://doi.org/10.1016/j.jhazmat.2007.10.039>
4. Cheradame H, Andreolety JP, Rousset E (1991) Synthesis of polymers containing pseudohalide groups by cationic polymerization. 1. Homopolymerization of 3,3-bis(azidomethyl)oxetane and its copolymerization with 3-chloromethyl-3-(2,5,8-trioxadecyl)oxetane. *Makromol Chem* 192(4):901–918
5. Zhang C, Li J, Luo YJ, Zhai B (2015) Preparation and property studies of carbon nanotubes covalent modified BAMO-AMMO energetic binders. *J Energ Mater* 33(4):305–314. <https://doi.org/10.1080/07370652.2014.990588>
6. Kubota N, Sonobe T, Yamamoto A, Shimizu H (1990) Burning rate characteristics of GAP propellants. *J Propul Power* 6(6):686–689
7. Frankel M, Grant L, Flanagan J (1992) Historical development of glycidyl azide polymer. *J Propul Power* 8(3):560–563
8. Nair JK, Satpute RS, Polke BG, Mukundan T, Asthana SN, Singh H (2002) Synthesis and characterisation of bis-azido methyl oxetane and its polymer and copolymer with tetrahydrofuran. *Defence Sci J* 52(2):147–156
9. Mohan YM, Mani Y, Raju KM (2006) Synthesis of azido polymers as potential energetic propellant binders. *Des Monomers Polym* 9(3):201–236. <https://doi.org/10.1163/15685506777351045>
10. Luo Y, Chen P, Zhao FQ, Hu RZ, Li SW, Gao Y (2004) Kinetics and mechanism of the thermal decomposition reaction of 3,3-bis(azidomethyl)oxetane/tetrahydrofuran copolymer. *Chin J Chem* 22(11):1219–1224
11. Miyazaki T, Kubota N (1992) Energetics of BAMO. *Propellants Explos Pyrotech* 17(1):5–9
12. Zhang C, Luo YJ, Jiao QJ, Zhai B, Guo XY (2014) Application of the BAMO-AMMO alternative block energetic thermoplastic elastomer in composite propellant. *Propellants Explos Pyrot* 39(5):689–693. <https://doi.org/10.1002/prop.201300164>
13. Manser GE, Ross DL (1981) Synthesis of energetic polymers. DTIC Document
14. Manser G, Guimont J, Ross D (1981) A new polymerization technique for preparing low molecular weight polyether glycols. *SR Int, Menlo Park*
15. Zhai JX, Yang RJ, Li JM (2008) Catalytic thermal decomposition and combustion of composite BAMO-THF propellants. *Combust Flame* 154(3):473–477. <https://doi.org/10.1016/j.combustflame.2008.04.016>
16. Cooper SL, Tobolsky AV (1966) Properties of linear elastomeric polyurethanes. *J Appl Polym Sci* 10(12):1837–1844
17. Janik H, Palys B, Petrovic ZS (2003) Multiphase-separated polyurethanes studied by micro-Raman spectroscopy. *Macromol Rapid Comm* 24(3):265–268. <https://doi.org/10.1002/Marc.200390039>
18. Romanova V, Begishev V, Karmanov V, Kondyurin A, Maitz MF (2002) Fourier transform Raman and Fourier transform infrared spectra of cross-linked polyurethaneurea films synthesized from solutions. *J Raman Spectrosc* 33(10):769–777
19. Ryan AJ, Willkomm WR, Bergstrom TB, Macosko CW, Koberstein JT, Yu CC, Russell TP (1991) Dynamics of (micro) phase separation during fast, bulk copolymerization: some synchrotron SAXS experiments. *Macromolecules* 24(10):2883–2889
20. Leung LM, Koberstein JT (1985) Small-angle scattering analysis of hard-microdomain structure and microphase mixing in polyurethane elastomers. *J Polym Sci B* 23(9):1883–1913
21. Garrett J, Runt J, Lin J (2000) Microphase separation of segmented poly (urethane urea) block copolymers. *Macromolecules* 33(17):6353–6359
22. Zia KM, Bhatti IA, Barikani M, Zuber M, Bhatti HN (2009) XRD studies of polyurethane elastomers based on chitin/1,4-butane diol blends. *Carbohydr Polym* 76(2):183–187. <https://doi.org/10.1016/j.carbpol.2008.10.005>



23. Trovati G, Sanches EA, Neto SC, Mascarenhas YP, Chierice GO (2010) Characterization of polyurethane resins by FTIR, TGA, and XRD. *J Appl Polym Sci* 115(1):263–268
24. Eceiza A, Martin M, De La Caba K, Kortaberria G, Gabilondo N, Corcuera M, Mondragon I (2008) Thermoplastic polyurethane elastomers based on polycarbonate diols with different soft segment molecular weight and chemical structure: mechanical and thermal properties. *Polym Eng Sci* 48(2):297–306
25. Camberlin Y, Pascault JP (1984) Phase segregation kinetics in segmented linear polyurethanes: relations between equilibrium time and chain mobility and between equilibrium degree of segregation and interaction parameter. *J Polym Sci Polym Phys Ed* 22(10):1835–1844
26. Mattia J, Painter P (2007) A comparison of hydrogen bonding and order in a polyurethane and poly(urethane-urea) and their blends with poly(ethylene glycol). *Macromolecules* 40(5):1546–1554
27. Yilgor I, Yilgor E, Guler IG, Ward TC, Wilkes GL (2006) FTIR investigation of the influence of diisocyanate symmetry on the morphology development in model segmented polyurethanes. *Polymer* 47(11):4105–4114
28. Ferry A, Jacobsson P, Van Heumen J, Stevens J (1996) Raman, infra-red and dsc studies of lithium coordination in a thermoplastic polyurethane. *Polymer* 37(5):737–744
29. Lee HS, Wang YK, Hsu SL (1987) Spectroscopic analysis of phase separation behavior of model polyurethanes. *Macromolecules* 20(9):2089–2095
30. Bonart R, Müller E (1974) Phase separation in urethane elastomers as judged by low-angle X-ray scattering. I. Fundamentals. *J Macromol Sci B* 10(1):177–189
31. Keicher T, Kuglstatter W, Eisele S, Wetzel T, Krause H (2009) Isocyanate-free curing of glycidyl azide polymer (GAP) with bis-propargyl-succinate (II). *Propell Explos Pyrot* 34(3):210–217. <https://doi.org/10.1002/prep.200900001>
32. Diaz E, Brousseau P, Ampleman G, Prud'homme RE (2003) Heats of combustion and formation of new energetic thermoplastic elastomers based on GAP, PolyNIMMO and PolyGLYN. *Propell Explos Pyrot* 28(3):101–106. <https://doi.org/10.1002/Prep.200390015>
33. Mathew S, Manu SK, Varghese TL (2008) Thermomechanical and morphological characteristics of cross-linked GAP and GAP-HTPB networks with different diisocyanates. *Propell Explos Pyrot* 33(2):146–152. <https://doi.org/10.1002/prep.200800213>
34. Yilgör I, Yilgör E, Wilkes GL (2015) Critical parameters in designing segmented polyurethanes and their effect on morphology and properties: a comprehensive review. *Polymer* 58:A1–A36
35. Tereshatov V, Makarova M, Senichev VY, Volkova E, Vnitskikh ZA, Slobodinyuk A (2015) The role of the soft phase in the hardening effect and the rate dependence of the ultimate physico-mechanical properties of urethane-containing segmented elastomers. *Colloid Polym Sci* 293(1):153–164
36. Tereshatov V, Makarova M, Tereshatova E (2004) Abnormal thermal and mechanical behavior of plasticized polyurethaneureas. *Polymer science Series A, Chemistry, physics* 46(12):1232–1238
37. Tereshatov V, Tereshatova E, Makarova M, Tereshatov S (2002) Influence of chemical structure and composition of mixed soft segments on the properties of elastomers with urethane-urea hard blocks. *Polym Sci Ser A* 44(3):275–281
38. Tereshatov V, Vnitskikh Z, Slobodinyuk A, Makarova M, Senichev V (2016) New multi-block isophorone diisocyanate-based copolymers with urethane urea hard segments. *J Elastomers Plast* 48(4):289–304
39. Lee HS, Hsu SL (1989) An analysis of phase separation kinetics of model polyurethanes. *Macromolecules* 22(3):1100–1105
40. Ishihara H, Kimura I, Saito K, Ono H (1974) Infrared studies on segmented polyurethane-urea elastomers. *J Macromol Sci B* 10(4):591–618
41. Paik Sung C, Smith T, Sung N (1980) Properties of segmented polyether poly(urethaneureas) based on 2, 4-toluene diisocyanate. 2. Infrared and mechanical studies. *Macromolecules* 13(1):117–121
42. Ning L, De-Ning W, Sheng-Kang Y (1997) Hydrogen-bonding properties of segmented polyether poly(urethane urea) copolymer. *Macromolecules* 30(15):4405–4409
43. Fedors RF (1974) A method for estimating both the solubility parameters and molar volumes of liquids. *Polym Eng Sci* 14(2):147–154
44. Koberstein JT, Stein RS (1983) Small-angle X-ray scattering studies of microdomain structure in segmented polyurethane elastomers. *J Polym Sci Polym Phys Ed* 21(8):1439–1472
45. Paik Sung C, Hu C, Wu C (1980) Properties of segmented poly(urethaneureas) based on 2, 4-toluene diisocyanate. 1. Thermal transitions, X-ray studies, and comparison with segmented poly(urethanes). *Macromolecules* 13(1):111–116

46. Yilgor I, Riffle J, Wilkes G, McGrath J (1982) Siloxane-urea segmented copolymers. *Polym Bull* 8(11–12):535–542
47. Stanford JL, Still RH, Wilkinson AN (2003) Effects of soft-segment prepolymer functionality on structure—property relations in RIM copolyurethanes. *Polymer* 44(14):3985–3994. [https://doi.org/10.1016/S0032-3861\(03\)000357-4](https://doi.org/10.1016/S0032-3861(03)000357-4)
48. Ertem SP, Yilgor E, Kosak C, Wilkes GL, Zhang M, Yilgor I (2012) Effect of soft segment molecular weight on tensile properties of poly (propylene oxide) based polyurethaneureas. *Polymer* 53(21):4614–4622
49. Sheth JP, Unal S, Yilgor E, Yilgor I, Beyer FL, Long TE, Wilkes GL (2005) A comparative study of the structure-property behavior of highly branched segmented poly(urethane urea) copolymers and their linear analogs. *Polymer* 46(23):10180–10190. <https://doi.org/10.1016/j.polymer.2005.07.068>